CMLS, Cell. Mol. Life Sci. 62 (2005) 1925–1937
1420-682X/05/171925-13
DOI 10.1007/s00018-005-5079-2

CMLS Cellular and Molecular Life Sciences

Review

Structural and dynamical features contributing to thermostability in α-amylases

J. Fitter

Forschungszentrum Jülich, IBI-2, Biologische Strukturforschung, 52425 Jülich (Germany), Fax: +49 2461 612020, e-mail: j.fitter@fz-juelich.de

Received 28 February 2005; received after revision 29 April 2005; accepted 19 May 2005
Online First 30 June 2005

Abstract. In recent years an increasing number of studies on thermophilic and hyperthermophilic proteins aiming to elucidate determinants of protein thermostability have yielded valuable insights about the relevant mechanisms. In particular, comparison of homologous enzymes with different thermostabilities (isolated from psychrophilic, mesophilic, thermophilic and hyperthermophilic organsims) offers a unique opportunity to determine the strategies of thermal adaptation. In this respect, the medium-sized amylolytic enzyme α-amylase is a well-established representative. Various studies on α-amylases with very different thermostabilities (melting temperature T_m = 40 –110 °C) report structural and dynamical features as well as thermodynamical properties which are supposed to play key roles in thermal adaptation. Here, results from selected homologous α-amylases are presented and discussed with respect to some new and recently proposed strategies to achieve thermostability.

Key words. Protein stability; protein unfolding; protein dynamics; thermal adaptation; unfolded states; conformational entropy.

Introduction

A vital property of most proteins is to maintain their native and in general unique structure under given environmental conditions. It has been demonstrated in many cases that the ability to build up and to maintain this native and functional structure within a particular range of temperature (or of pH, pressure, salinity) is an intrinsic property of the protein itself which is determined by the amino acid sequence [1]. According to the very different habitats in which the organisms thrive, the temperature range where the native structure is present can vary significantly [2–4]. In particular, psychrophilic (cold adapted) and thermophilic or hyperthermophilic (heat adapted) organisms are important sources of proteins which can be used as prototypes in comparative investigations to study the determinants of structural stability under extreme conditions [5–7]. Numerous comparative studies of homologous proteins, mainly from mesophilic and thermophilic sources [8–16], but in some cases also psychrophilic [17, 18] sources have been performed. The question especially of how proteins deal with extreme temperatures (thermal adaptation) is not only related to thermostability, but also to a proper functionality of the proteins at given temperatures.

Native and functional protein structures are held together by a subtle balance of non-covalent forces or interactions, such as H bonds, ion pairs, and hydrophobic and van der Waals interactions. At elevated temperatures these non-covalent interactions are too weak or become counterbalanced by other interactions, and proteins start to unfold. Protein unfolding can be observed by many different techniques, including differential scanning calorimetry (DSC), fluorescence, circular dichroism (CD), Fourier transform infrared (FTIR) and nuclear magnetic resonance (NMR) spectroscopies, and sedimentation techniques (see

for example [19–21]). The melting temperature, T_m, as determined by calorimetry and spectroscopic techniques, is typically the same as measured by the above-mentioned experimental approaches. In most cases the loss of secondary and tertiary structure is concomitant with enzyme inactivation at high temperatures. Small monomeric proteins commonly unfold via a two-state transition, where the unfolding intermediate states are not or barely accumulated. Some proteins regain their native and functional structure upon cooling. From this kind of unfolding, a so-called thermodynamically reversible unfolding, the thermodynamic parameters that characterize the transition can be determined. Larger multi-domain proteins, however, generally exhibit a different behavior. It is assumed that, mainly, exposed hydrophobic and charged residues are responsible for the fact that proteins, in particular the unfolded states, form aggregates. These aggregates often result in irreversible unfolding. In this case the characterization of the unfolding process in terms of thermodynamic parameters is not straightforward and has been attempted only in rare cases [22, 23].

Various determinants of protein stability and proposed mechanisms for how proteins achieve sufficient structural stability under extreme environmental conditions have been reported. Thermostability appears to be conferred by a variety of strategies. Numerous structural strategies, a greater number of ionic interactions, disulphide bridges and prolines, a greater extent of hydrophobic-surface burial, as well as improved core packing, shorter surface loops and higher states of oligomerization have all been proposed and at least partly proven to be responsible for increased thermostability (see for example [5–7]). Interestingly, for nearly all the described structural strategies, counter-examples (for other sets of homologous proteins) can be found where the specific mechanism is not observed or utilized [24]. Thus, many different forces and interactions may and often do contribute to thermal stability. The challenge is to pinpoint which of the different factors and interactions are the most critical for the specific proteins [25]. In order to attain this goal not only factors directly related to structural properties, as mentioned above, but also dynamical properties (structural flexibility

Table 1. List of selected homologous α-amylases for which the 3D structures have been solved and their thermostability properties have been identified.

Origin	PDB entry	No. of residues	MW [kDa]	No. of Ca ions	Add. /other ions	No. of SS bridges (no. cys.)	T_m [°]
Alteromonas haloplanctis (AHA) psychrophile	1AQH	453	49.358	1	1Cl	4(8)	44
Pig pancreatic (PPA) mesophile	1DHK	496	55.357	1	1Cl	4(12)	65
Aspergillus oryzae (TAKA) mesophile	6TAA	478	52.490	2	–	4(9)	71
Bacillus subtilis (BSUA) mesophile	1BAG	619	68.421	3	–	0(1)	83
Bacillus amyloliquefaciens (BAA) thermophile (mesophile)	1E43	483	58.843	4	1Na	0	86
Bacillus licheniformis (BLA) thermophile (mesophile)	1BLI	483	58.274	3	1Na	0	102
Pyrococcus woesi/furiosus (PWA)/(PFA) hyperthermophile	1MXG	435	50.175	1	Zn, 3Mg	2(5)	~110

The given melting temperatures have been determined under calcium-saturated conditions. The X-ray structure assigned to the α-amylase from *Bac. amyloliquefaciens* (PDB entry 1E43) has been solved from a chimeric fusion construct consisting of residues 1–300 from BAA and 301–483 from BLA[40]. *Bac. amyloliquefaciens* and *Bac. licheniformis* are both mesophilic organisms but contain very thermostable α-amylases which are therefore often denoted as thermophilic enzymes. The α-amylase from the hyperthermophilic archaeon *Pyrococcus woesi* (PWA), is identical to the extracellular α-amylase from *Pyrococcus furiosus* (PFA), for which the given stability properties have been determined [42, 43]. Another intracellular α-amylase from *Pyrococcus furiosus* (which will not be discussed here) has a larger molecular mass (76261 Da), but shows a rather similar thermostability compared with the intracellular PFA [41, 42].

of the protein) and features of the unfolding transition (e.g., rate constants of the unfolding and refolding transition, reversibility of the transition etc.) are worth studying in detail.

In principle, even mesophilic proteins can be extremely thermostable, and the task of elucidating determinants of thermostability is not confined to studies of proteins from extremophiles (see table 1). However, there are often two primary motivations for studying thermophilic and hyperthermophilic proteins. Besides an academic interest in ascertaining the major attributes and mechanisms of how proteins achieve extreme thermostability, thermophilic proteins have attracted increasing attention because of their potential use in biotechnology processes [7]. The starch-degrading enzyme α-amylase plays an important role in both fields of interest [26–28]. α-Amylase (1,4-α-D-glucan glucanohydrolase EC 3.2.1.1) catalyzes hydrolysis of α-1,4-glucosidic linkages of starch [26]. It is found in eubacteria as well as in eukaryota and has a huge variation in temperature and pH optima. Bacterial and fungal α-amylases, and in particular the enzymes from the *Bacillus* species, are of special interest for large-scale biotechnology processes due to their remarkable thermostability and because efficient expression systems are available for these enzymes. Enzymes with α-amylase activity are found in two structurally different glycoside hydrolase families (family 13 and 57; for more details see [29] and references therein). α-Amylases have been isolated from various organisms (psychrophilic, mesophilic, thermophilic, hyperthermophilic) and show an extremely broad range of melting temperatures (40–110 °C). Over the last 2 decades this monomeric multi-domain protein (50–70 kDa) has become an important model system for investigating thermal adaptation of medium-sized enzymes [29–33].

In this review studies are reported that investigate molecular mechanisms and determinants of thermostability and thermal adaptation in the case of α-amylases. By way of example, seven homologous α-amylases with different thermostabilities were chosen for a comparative analysis. Besides well-approved features which are known to play an important role for the thermostabilization of α-amylases, further properties such as structural flexibility and properties of the unfolded states as well as of the unfolding transition will be discussed with respect to their impact on thermostability.

Structural properties of the native state

Most of the known α-amylase structures consist of a monomer with three domains exhibiting an (β/α)-barrel (domain A) as a central structural unit. A listing of intensively studied α-amylases for which a three-dimensional (3D) structure has been solved (see fig. 1) is given in table 1. Domain B, which together with the central domain A forms the substrate binding cleft, and domain C are located at opposite sites of the central TIM-barrel. In contrast to the central part of the structure, domains C and B vary in size and structure among the α-amylases. Furthermore, nearly all known α-amylases have at least one conserved calcium binding site. Most of the known α-amylases have even more calcium binding sites, which contribute substantially to the structural stability [34–39]. As shown in table 1, selected α-amylases vary dramatically with respect to their individual thermostabilities. Although the corresponding 3D structures appear rather homologous at first, various proposals on the stabilizing role of structural features have been reported for the individual α-amylases [35, 37, 40–44]. In several studies specific locations in the protein structures have been identified which are relevant for thermostability. Comparative studies on various mutants of *Bacillus licheniformis* α-amylase (BLA) [45, 46], of *Bacillus amyloliquefaciens* α-amylase (BAA) [47] and of PFA [48] have demonstrated that mutation of individual residues either increases or decreases overall thermostability. A detailed overview about these features was also given by Nielsen et al. [30].

More general stabilization features, such as oligomeric state, number of disulphide bridges, number of bound divalent ions, or the number and volume of cavities (compactness), do not show a correlation with thermostability throughout the set of homologous α-amylases presented in table 1. With the exception of *Alteromonas haloplanctis* α-amylase (AHA) [35], all α-amylases discussed here are

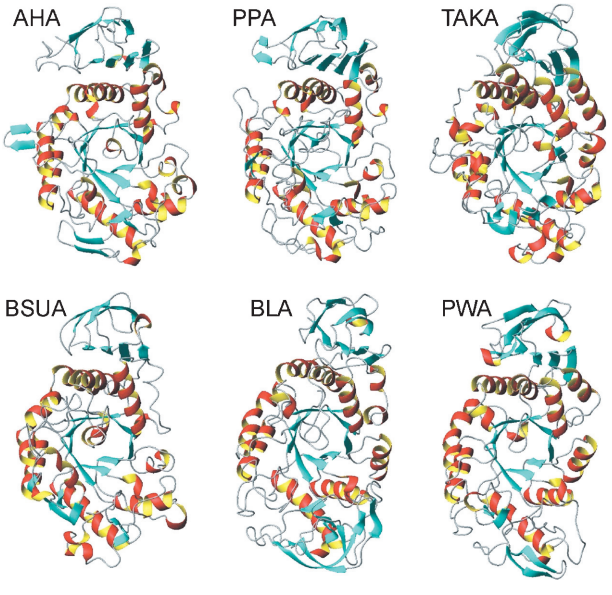

Figure 1. Three-dimensional structures of various α-amylases (see table 1) as determined by X-ray crystallography. The structures were produced using the program *MOLMOL* [88]. For simplicity, the bound ion atoms (Ca, Cl, Na, Zn etc.) are not shown.

Table 2. The effect of calcium on thermostability in terms of melting temperatures is given here.

Enzymes	T_m [°C] Ca saturated	T_m [°C] Ca depleted	ΔT_m [°C]
AHA	44	44	0
PPA	65	48	17
TAKA	71	57	14
BSUA	83	46	37
BAA	86	38	48
BLA	102	52	50
PWA/PFA	~110	n.d.	n.d.

The data were taken from the following references. AHA and PPA [35]; TAKA [36]; BSUA, Fitter et al., to be published; BAA and BLA [37]; for PWA/PFA, only thermoinactivation data are available [42, 48, 50]; for the most similar intracellular PFA see [41].

stabilized by calcium at elevated temperature. As shown in table 2, the difference in melting temperatures, ΔT_m between calcium-saturated and calcium-depleted samples varies in the range from 14 up to 50 °C. For the most homologous pair of α-amylases, namely BAA and BLA (81% identity, 88% similarity [44]), this difference is extremely large, at about 50 °C, and nearly identical for both enzymes. Although calcium exerts this strong influence on the thermal stability of both enzymes, the specific difference in thermostability between BAA and BLA (~15 °C) is the same with and without calcium and seems not to be related to the calcium binding properties, but appears to be an intrinsic property of the protein structures themselves [49]. The *Bacillus subtilis* α-amylase (BSUA) exhibiting three calcium binding sites, like BLA, shows a ΔT_m of 37 °C upon calcium binding, while Taka α-amylase A (TAKA) (two calcium ions) and pig pancreatic α-amylase (PPA) (one calcium ion) show much smaller ΔT_m values. With respect to these examples, the number of binding sites seems to show at least a tentative correlation with respect to the difference in thermostability between calcium-saturated and -depleted α-amylase samples. Early studies on PWA/PFA at room temperature demonstrated that Ca^{2+} is not required for stability [42, 50] which gave rise to the assumption that calcium is not essential for thermostabilization of this enzyme. However, a more recent study indicates that calcium is required for PFA thermostability at elevated temperatures, while below 75 °C it is not required [48]. The role of other ions for structural stabilization appears to be less important, but is on the other hand less well investigated. It is assumed that zinc at least participates in the thermostabilization of PFA [48]. From structural analyses on BLA and on BAA it is well known that both enzymes exhibit a unique Ca-Na-Ca metal triade at the interface between the A and B domains [40, 51]. Therefore, sodium seems to play an essential role for stabilizing BAA and BLA, since the sodium-free buffers exhibit a T_m value 20 °C below that of samples with sodium under calcium-saturated conditions [49]. Recently, the structure of a α-amylase from *Bacillus* sp. (AmyK38) was solved. This structure has no calcium ions, but at least two sodium ions replace the calcium and play an important role in retaining the structure [52].

Temperature dependence of enzymatic activity

In various studies the enzymatic activity of several α-amylases was measured as a function of temperature. One use of these measurements is to determine the temperature of maximal enzymatic activity (T_{opt}), which is an important parameter in characterizing the thermal adaptation process [23, 37, 42]. The temperature dependence and the apparent T_{opt} principally depend on the procedures used to assay enzymatic activity (buffers, heat rate and incubation times, thermostability of the substrate etc.; see for example [53]). However, temperature-dependent activity plots with data taken from the literature allow at least a qualitative comparison (see fig. 2). As expected, the temperature of maximal activity is clearly related to the thermostabilities of the selected α-amylases. Typically the observed T_{opt} values are 5–15 °C below the melting temperatures. Interestingly, BLA, and particularly BAA, displays a rather high enzymatic activity far below T_{opt} which seems to be related to the fact that the sources of theses rather thermostable enzymes are mesophilic organisms (see table 1). In contrast, AHA, PPA and PWA appear to be adapted to a much narrower temperature range.

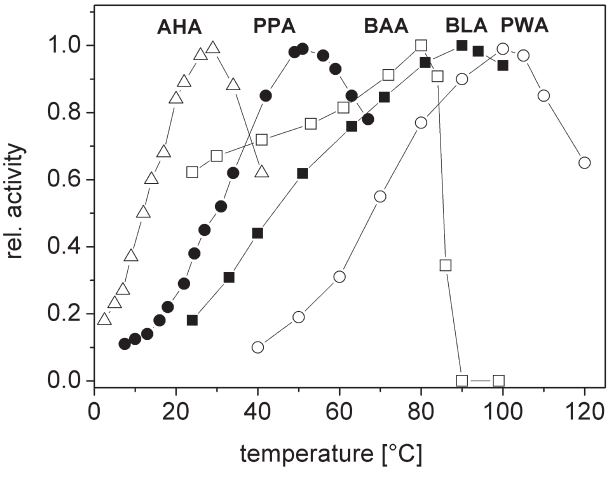

Figure 2. The temperature dependence of enzymatic activity as measured for various α-amlyases (see table 1). The temperature of the greatest enzymatic activity can be attributed as an apparent T_{opt}. The data were taken from the following references. AHA (T_{opt} = 30 °C) and PPA (T_{opt} = 50 °C), [23]; BAA (T_{opt} = 80 °C) and BLA (T_{opt} = 90 °C), [37] and PWA/PFA (T_{opt} = 100 °C), [42].

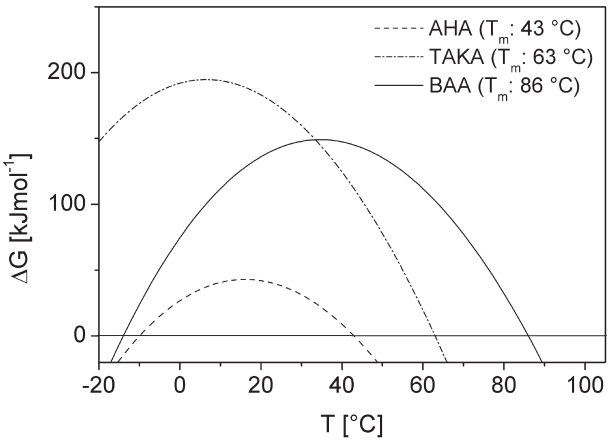

Figure 3. Presentation of protein stability curves as a function of temperature calculated on the basis of data as published in the literature [35, 36] using the modified Gibbs-Helmholtz equation: $\Delta G(T) = \Delta H_m \cdot (1 - T/T_m) + \Delta C_p[T - T_m - T \cdot \ln(T/T_m)]$. The following thermodynamic parameters were used: AHA: ΔCp, 35.4 kJ K^{-1} mol^{-1}; T_m, 316 °K; ΔH_m, 995.8 kJ mol^{-1}; TAKA: ΔCp, 36.4 kJ K^{-1} mol^{-1}; T_m, 336 °K; ΔH_m, 2250 kJ mol^{-1}; (here a T_m of 63 °C was obtained for samples without additional calcium) BAA: ΔCp, 36.0 kJ K^{-1} mol^{-1}; T_m, 359 °K; ΔH_m, 2037.7 kJ mol^{-1}.

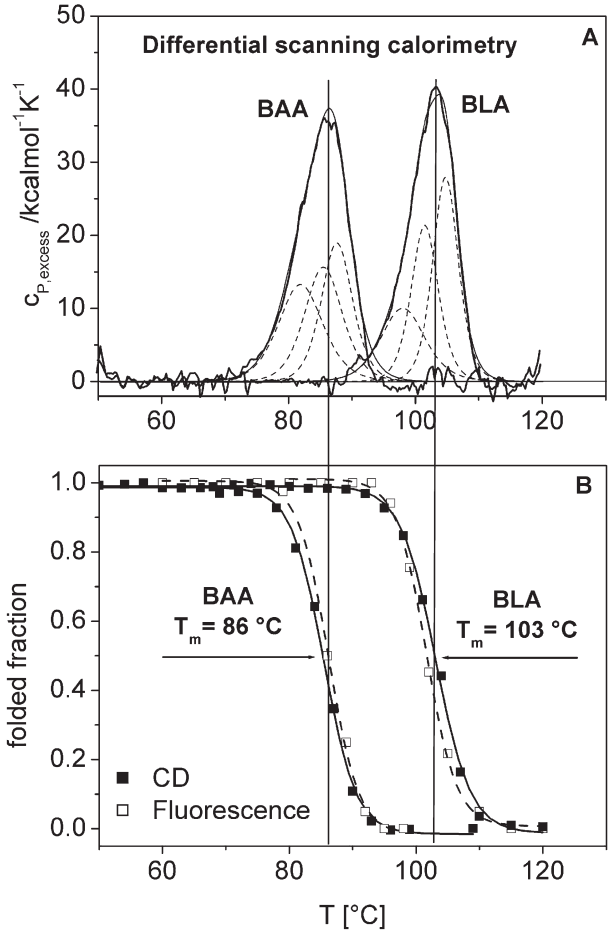

Figure 4. Thermograms measured using DSC (*A*) and spectroscopic data (*B*) displaying the thermal unfolding transition for BAA and BLA. The single peaked DSC data can be deconvoluted into three nearly cooperative transitions, represented by Gaussian curves (dashed lines). The CD data were measured in the far UV region, and the intensity as measured at 222 nm is shown as a function of temperature. The tryptophan fluorescence signal was obtained from a red shift of the fluorescence emission spectra with peak maxima between 336 nm (folded state) and 341 nm (unfolded state). The data were taken from [37, 49].

The unfolding transition

Spectroscopic and microcalorimetric studies reveal detailed insights in the unfolding transitions of several α-amylases. While CD spectroscopy monitors the integrity of secondary structural elements, tryptophan fluorescence spectroscopy can be used to measure the 3D compactness of a protein. In contrast to spectroscopic techniques which only report on protein properties during the unfolding transition, differential scanning calorimetry measures the change of heat capacities (ΔCp), which also includes contributions from the surrounding solvent (e.g., rearrangement of hydration water).

The stability of proteins is primarily characterized by their thermodynamic stability, which in the most general case is determined by the difference in the free energy, ΔG, between the folded (N) and the unfolded (U) state ($\Delta G = \Delta H - T\Delta S$). In the simplest case a two-state model with a reversible unfolding transition is applied to determine thermodynamic parameters at the thermodynamic equilibrium. The temperature dependence of ΔG allows deeper insights into mechanisms of how thermostability is achieved. Since protein unfolding is known to be accompanied by a non-zero ΔCp, the Gibbs-Helmholtz plots (parabolic stability curves in fig. 3) are distinctly non-linear, and one observes thermal unfolding at high temperatures (T_m at $\Delta G = 0$) as well as at low temperatures ('cold denaturation' point). These plots give valuable information about enthalpic contributions (ΔH change of enthalpy), often related to the structural stability of a protein, and entropic contributions (ΔS change of entropy), which have also been shown to play a role in reaching high thermostabilities [9, 54]. Examples of stability curves are shown for three different α-amylases in figure 3. The comparison between TAKA and BAA demonstrates that high thermodynamic stability at room temperatures (i.e., large maximal ΔG) is not necessarily related to high thermostability (or thermal stability, i.e., a high T_m). However, in another example where AHA is compared with BAA or with TAKA, a large maximal ΔG is related to thermostability.

The unfolding transition as monitored by the above-mentioned techniques often appears to be rather cooperative, which is demonstrated in figure 4 for BAA and BLA. With respect to the applied heating rate of approximately 1 °C per minute, both enzymes exhibit a transition

width of about 20 °C. Similar rather cooperative transitions have been observed at their corresponding melting temperatures for other α-amylases, namely, AHA, PPA and TAKA [35, 36]. With the exception of AHA, all α-amylases studied so far exhibit an irreversible unfolding transition. In addition to a remarkably high reversibility (99%) for a 50-kDa multi-domain protein, AHA displays a much narrower transition width (~10 °C transition width at 1 °C/min heating rate), and shows all the attributes of a pure two-state unfolding transition [35]. The irreversible unfolding transitions, as generally observed for mesophilic and thermophilic α-amylases under in vitro conditions, are mainly caused by aggregation of the enzymes in the unfolded state at elevated temperature. A simple model that considers irreversible steps in the thermoinactivation process is given by the Lumry-Eyring model [55]:

$$N \underset{K_f}{\overset{K_u}{\leftrightarrow}} U \overset{K_i}{\rightarrow} D$$

Here N is the native state, U is the unfolded state and D stands for the final denatured state. However, in some cases thermodynamic parameters have been determined on the basis of equilibrium studies where the irreversible steps were assumed to have slower rates than the reversible steps [23, 35–37]. Such results should, however, be taken with caution, because small changes in the obtained thermodynamic parameter (e.g., ΔCp) may have large effects in the corresponding stability curves (see fig. 3).

Table 3. For the three most thermostable α-amylases, the half-life periods as measured at different temperatures near the temperature of maximal enzymatic activity (for T_{opt} values see fig. 2) are given.

	T [°C]	Half-life periods: $t_{1/2}$	Conditions
BAA	80	50 min	pH ~7; 1 mM CaCl[#]
T_{opt} = 80 °C	90	2 min	pH ~7; 1 mM CaCl[&]
BLA	90	250 min	pH ~7; 1 mM CaCl[*,#]
T_{opt} = 90 °C	95	20 min	pH ~7; 1 mM CaCl[§]
PWA/PFA	100	>12 h	pH 4.5; no add.Ca^{2+}[$]
T_{opt} = 100 °C	110	4 h	pH 4.5; no add. Ca^{2+}[$]
	120	2 h	pH 4.5; no add. Ca^{2+}[$]

The data were taken from the following references. [#], [37]; [§], [59]; [*], [60]; [&], [45]; [$], [42].

thermostability of proteins [37, 42, 45, 59, 60]. For BAA, BLA and PFA, the half-life periods of residual enzymatic activity, as measured at elevated temperatures, are given in table 3. The most interesting feature here is that enzymes with a higher thermostability exhibit their enzymatic activity of longer duration at elevated temperatures, compared with less thermostable enzymes. This seems to support a kinetic stabilization mechanism in the case of the selected α-amylases.

Depending on the protein concentration and taking into account much longer time scales, significant unfolding can also occur below the apparent melting temperature (see

Inactivation and unfolding kinetics

Most studies determining the thermostability of proteins are performed under equilibrium conditions. However, the use of kinetic studies can reveal additional interesting features of thermostability, particularly for transitions with irreversible steps. Following transition state theory, not only ΔG but also the barrier height of the transition state determines the folding and unfolding rates and therefore controls protein stability with respect to the corresponding time regime. Recently it was demonstrated in some cases that a higher thermostability was accompanied by significantly smaller unfolding rates (K_u) as compared with their mesophilic homologues [8, 56–58]. In contrast, at least for proteins with reversible unfolding, only small differences in the (re-)folding rates (K_f) were observed [56]. This reveals that a low K_u value may be a key feature in kinetically protecting the native state of thermophilic proteins (kinetic stabilization).

In this respect, for α-amylases mainly studies on thermo-inactivation kinetics are available from the literature. Although the thermo-inactivation does not occur necessarily at the same temperature at which the structural unfolding transition takes place (see table 1, fig. 2 and [23]), this approach is quite often used to characterize the

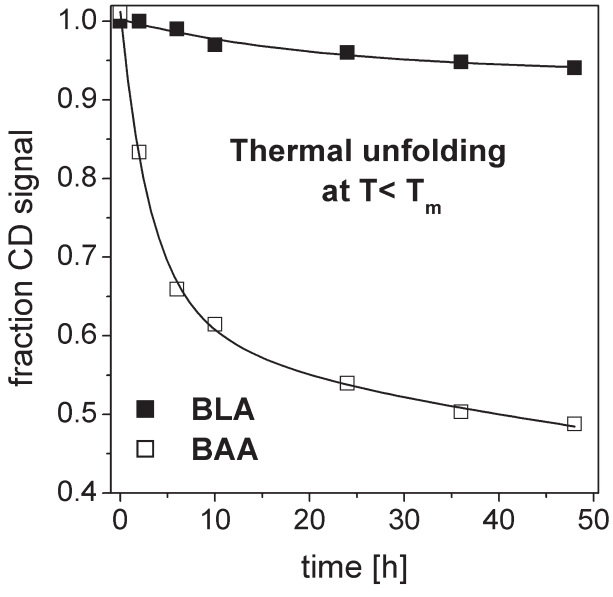

Figure 5. Long-term stability of samples in 2 mM EDTA buffer as measured with CD spectroscopy at 25 °C (data taken from [49]). For these calcium-depleted samples the following melting temperatures have been determined: T_m = 38 °C for BAA and T_m = 52 °C for BLA (see table 2).

for example [61]). An example of such behavior is given in figure 5 for BAA and BLA. The melting temperature of BLA under calcium-depleted conditions is approximately 27 °C higher than the room temperature (25 °C) at which the measurements were performed (see table 2). Therefore, only a very small amount of BLA (5%) was unfolded after 2 days. In contrast, BAA has a melting temperature which is only 13 °C above room temperature. Taking into account the transition width for the unfolding transition of BAA (±10 °C, see fig. 4), BAA starts to unfold even at room temperature. Due to irreversible aggregation of the unfolded state (see the Lumry-Eyring model) and considering long time scales of the corresponding measurements, the unfolded state is cumulative. As a result, one obtains 50% unfolded BAA after 2 days at room temperature. This example demonstrates that an operative stability strongly depends on the relation of the different rates (K_u, K_f, K_i) in the Lumry-Eyring equation and on the protein concentration (for more details see also [61]).

Properties of the unfolded state

It is obvious from basic principles that not only properties of the folded state but also properties of the unfolded state have an impact on protein stability and on the unfolding transition. One property which is more or less directly related to the conformational entropy of the unfolded state is given by structural compactness. In general, a native protein structure is efficiently packed and appears considerably compact. The native protein exhibits a rather restricted conformational freedom, at least in the interior of the structure. Upon unfolding, a larger degree of conformational freedom is accompanied by less compact structures. The increase in size of expanding protein structures can be monitored by the use of tryptophan fluorescence spectroscopy or by dynamic light scattering. The fluorescence emission intensity, which in many cases peaks at wavelengths λ_{max} between 330 and 340 nm for the native state, shows a typical decrease in signal intensity with increasing temperature. At the unfolding transition one observes an additional decrease in signal intensity and a characteristic red shift ($\Delta\lambda_{max}$ ~5–20 nm) of the emission peak. These red shifts, which have been observed for many proteins during the unfolding process, are caused by an increased solvent accessibility of tryptophan residues as provided in the fully unfolded state [62]. Fully accessible tryptophan residues reveal an emission spectrum which peaks around 350 nm. In comparative studies the fluorescence emission red shift can be used to follow the structural expansion of the protein structure during the unfolding process. For BAA, BLA and TAKA, thermal unfolding and denaturant-induced unfolding (8 M GndHCl) was analyzed using this approach (see fig. 6).

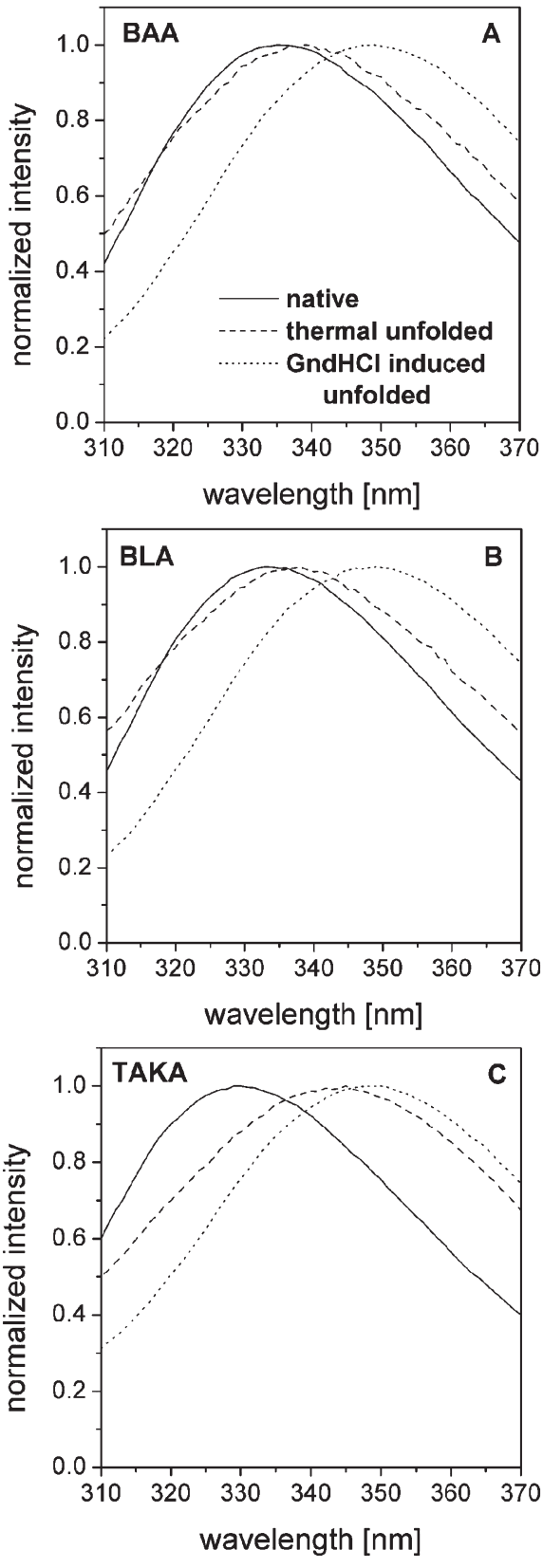

Figure 6. Normalized fluorescence emission spectra for the folded (solid lines) and for unfolded (thermal unfolded, dashed lines, GndHCl induced, dotted lines) states as measured with $\lambda_{exc.}$ 280 nm. The data were taken from [49].

For BAA and BLA, thermal unfolding is characterized by rather small red shifts ($\Delta\lambda_{max}$ ~ 4–5 nm), while denaturant-induced unfolding reveals much larger red shifts of about 15 nm [49]. In contrast, the less thermostable TAKA α-amylase exhibits a much larger red shift of about 10 nm upon thermal unfolding and a similar red shift for denaturant-induced unfolding. In general, more compact unfolded states, indicated by smaller red shifts for thermally unfolded BAA and BLA as compared with TAKA, lower the conformational entropy ΔS between the folded and unfolded state. This can have a stabilizing effect with respect to thermal unfolding. For BAA and BLA, structural expansion upon denaturant-induced unfolding was also measured by dynamic light scattering (DLS) [49]. The corresponding hydrodynamic radii are rather similar for both folded states (3.2 nm) and differ for the fully unfolded state, with 5.2 nm for BLA and 6.1 nm for BAA. Thermally unfolded proteins exhibit strong aggregation, which makes it impossible to measure hydrodynamic radii for monomeric proteins. For both BLA and BAA, the secondary structural elements (measured using CD spectroscopy) completely disappear on thermal and denaturant-induced unfolding. On the basis of current data, it is not yet possible to say to what extent the compactness of unfolded states has an impact on the thermostability of α-amylases. Interestingly, in the case of several other proteins (thermophilic single-domain proteins), results indicate that compactness and 'residual native structures' in the unfolded state play a role in thermostabilization [63–65].

The role of structural fluctuations and protein flexibility

Temperature exerts a profound influence on the balanced interplay of structural flexibility and rigidity. Although folded proteins exhibit a certain rigidity that maintains their unique 3D structure, conformational fluctuations are, nevertheless, present in the native state. Often these fluctuations are required for proper functioning [66–69]. One of the motivations for performing comparative studies on the dynamic properties of homologous proteins with different thermostabilities, is the perception that thermostable proteins should have more rigid structures as compared with mesophilic or even psychropilic proteins. The 'corresponding state hypothesis' argues that proteins show a similar structural flexibility at their adapted temperature [70]. As a consequence, thermophilic proteins exhibit reduced flexibility at room temperature and appear more rigid compared with mesophilic or psychrophilic proteins. This correlation between thermostability and rigidity of protein structures has been observed in various studies [71–75]. A comparison of protein flexibility between homologous proteins was studied by measuring structural dynamics using FTIR (H/D exchange kinetics) [71, 76], dynamic quenching of tryptophan fluorescence [23, 49, 74, 75], NMR [77, 78] and neutron spectroscopy [73, 76], as well as molecular dynamics (MD) simulation techniques [10, 72, 79]. All techniques can be utilized to probe internal structural fluctuations, but they are very different with respect to time scales and to amplitude of motion. The NMR technique clearly has the best potential for detailed experimental investigation of motion on different time scales and with a spatial resolution which cannot be reached by any other of the above-mentioned techniques. But it is limited to smaller proteins structures. With respect to several dynamics studies of homologous α-amylases, the results revealed are rather divers. A comparative analysis of AHA, PPA and BAA using fluorescence quenching supports the concept of corresponding states [23]. It was found that a decreasing quenching efficiency, indicative for increasing protein rigidity, was correlated to increasing thermostability (AHA $\rightarrow$ PPA $\rightarrow$ BAA). In another case of comparative studies of BAA and BLA, three different techniques were employed. With respect to amide-proton exchange kinetics (fig. 7A) BLA shows larger exchange rates and larger fractions of exchanged protons compared with BAA, which is indicative of a more flexible BLA structure, at least with respect to faster exchange processes. On a longer time scale the exchange rates of both enzymes are quite similar. Fluorescence quenching (fig. 7B) shows no difference between BLA and BAA. The observed amide-proton exchange kinetics are generally related to conformational changes which appear rather infrequently and can be attributed as slower motion. A certain cooperativeness of several local and faster fluctuations is required to make an amide-proton inside the protein structure accessible to solvent molecules. Fluorescence quenching is not explicitly related to a certain time scale, but like amide-proton exchange, it depends on the accessibility of special groups (tryptophan residues), often also located in the interior of the protein. Therefore, this technique also probes fairly slow structural fluctuations. A much more direct measure of internal protein dynamics is given by neutron spectroscopy. Incoherent neutron scattering (INS) makes use of a large incoherent cross-section of hydrogen nuclei (~40 times larger than incoherent cross-sections of other elements in biological samples), and is well suited to study internal molecular motions in a time range from sub-picoseconds to nanoseconds [80, 81]. According to the diffusive and liquid-like character of most motion in proteins, one mainly observes an elastic scattering amplitude (A_0) and a quasielastic scattering amplitude (A_1) (see fig. 8A). Figure 7C shows the Q-dependence (Q is related to an inverse amplitude of motion) of the elastic scattering amplitude (normalized to unity with $A_0 + A_1 = 1$). The Q-dependence of A_0 looks qualitatively quite similar for all measurements. Because we observe localized fluctuations, mainly reorientational

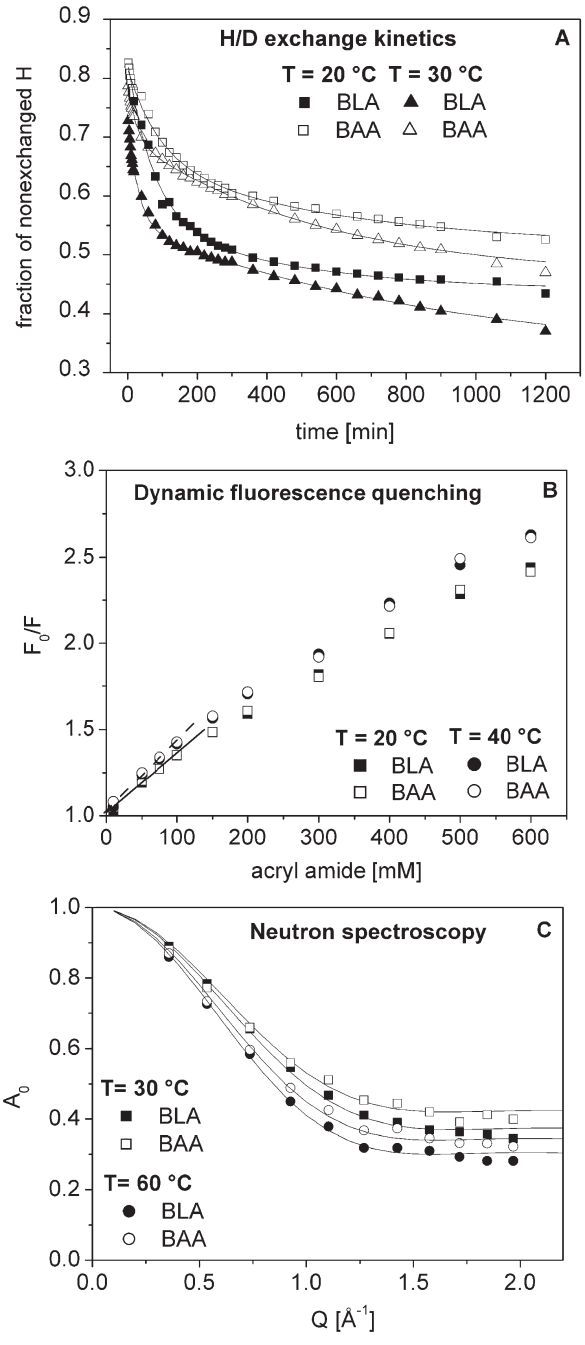

Figure 7. (*A*) Normalized fractions of non-exchanged amide protons as a function of exposure time with D_2O solvent measured with BLA and BAA for 20 and 30 °C. The experimental data points have been obtained from amide II intensities (at 1550 cm^{-1}) as detected by FT-IR spectroscopy (data from [76]). (*B*) Stern-Volmer plots of tryptophan fluorescence quenching by acryl amide. The collision quenching constant, K_{sv}, values determined in the region up to 100 mM are given by the slope of the fitting line. They are identical for BLA and BAA within the limits of error (3.37 M^{-1} at 20 °C and 3.84 M^{-1} at 40 °C; data from [49]). (*C*) Elastic incoherent structure factors as a function of neutron momentum transfer, Q, for BLA and BAA as measured with protein solutions at 30 and 60 °C. The normalized structure factors, A_0, have been calculated from elastic (zero energy transfer $\hbar\omega = 0$ within the given energy resolution) and quasielastic (nonzero energy transfer $\hbar\omega \neq 0$) scattering contributions as shown in the energy transfer spectra (see fig. 8A). The data were taken from [37].

movements of polypeptide side groups, A_0 starts at its maximum value (i.e., unity) in the low Q-range. A decrease of A_0 with increasing Q, more precisely the slope of A_0 versus Q, is related to motion with average amplitude in the range between 1 and 3 Å. Above Q = 1.5 $Å^{-1}$ a constant level with A_0-values between 0.4 and 0.3 is reached. These values give the fraction of hydrogens (normalized to unity) in the protein structure not participating in motion visible within the resolution limits of the spectrometer. The complementary fraction of hydrogens directly reflects the conformational flexibility of the enzyme. As expected, the data from measurements performed at 60 °C show smaller A_0 values and therefore a higher conformational flexibility as compared with the 30 °C data. Interestingly, for both temperatures BLA shows smaller A_0 values compared with BAA, indicating a higher conformational flexibility for BLA. Within the limits of error, these differences (at high Q, A_1 values are ~6–7% larger for BLA) are the same for both temperatures. Although theses differences are small, they are significant and fully reproducible [37, 76]. As a result, we conclude that the example of BLA and BAA does not support the corresponding state hypothesis.

It is still a matter of debate to what extent the corresponding state hypothesis is implemented and valid in thermal adaptation processes. Possibly the major features and effects are only visible between proteins from quite different (i.e., psychrophilic, mesophilic, thermophilic) sources. In this case typical features would not be observable for two rather thermostable proteins originating from organisms which are not adapted to very different temperatures (both, BAA and BLA, are from mesophilic sources). However, other examples in the literature reveal similar results which also do not support the corresponding state hypothesis [77–79]. Another important aspect in this context is related to the fact that motion does occur on different time scales with different amplitudes and located in different parts of an enzyme. Some of this motion might be related to enzymatic activity; some might be related to a pre-stage of an unfolding process and thus most probably plays a role in protein stability. Therefore, the role of structural fluctuations in thermal adaptation is most probably manifold and complex [78], and most of the techniques applied cover only a very limited portion of the motion occurring in protein structures.

With respect to the possible impact of internal fluctuations on thermostability, additional flexibility can stabilize the native state of a protein under certain conditions. In general, conformational motion which is related to the unfolding pathway can destabilize the native state. Therefore, hindrance or suppression of this motion by additional hydrogen bonds or salt-bridges will stabilize the structure. This is an example of enthalpic stabilization. Moreover, conformational fluctuations can also increase the confor-

mational entropy of the folded state with respect to the unfolded state. A resulting change of conformational entropy during unfolding, ΔS, will be smaller, and increased flexibility (of the folded state) has a stabilizing effect (see above). Therefore, the larger conformational flexibility on the picosecond time scale observed for BLA as compared with BAA is not contradictory to their corresponding thermostabilities (see fig. 7C). In order to demonstrate that entropic stabilization does indeed play a role, one has also to measure the structural fluctuations of the unfolded states. In the case of BLA, the dynamical properties for both states are presented in figure 8. As expected, the unfolded state is much more flexible compared with the more compact folded state at the same temperature (fig. 8A, B). With increasing temperature for both states, the structural fluctuations become more pronounced (steeper decrease of A_0 with Q, see fig. 8C) at higher temperatures. The important feature here is that the unfolded state shows a more pronounced increase in fluctuation with rising temperature as compared with the folded state. As a consequence, ΔS increases more and more at elevated temperatures, which is at least partly responsible for the downward curvature of the stability plots shown in figure 3. The fact that at elevated temperatures ΔS (more precisely $T\Delta S$) becomes larger than the enthalpic term ΔH is the reason for thermal unfolding. In principle, not only conformational entropy arising from the protein structure contributes to ΔS, but so does the hydration water. However, the measure of the protein dynamics for the folded and unfolded state at different temperatures allows the calculation of entropy changes during heating (for further details see [82]). Only further studies with other α-amylases can meaningfully determine whether and to which extent the conformational entropy of the protein structure contributes to the different thermostabilities of homologous α-amylases. Unfortunately, measuring of dynamics with samples in the unfolded state is a difficult task due to strong aggregation of these states at elevated temperatures.

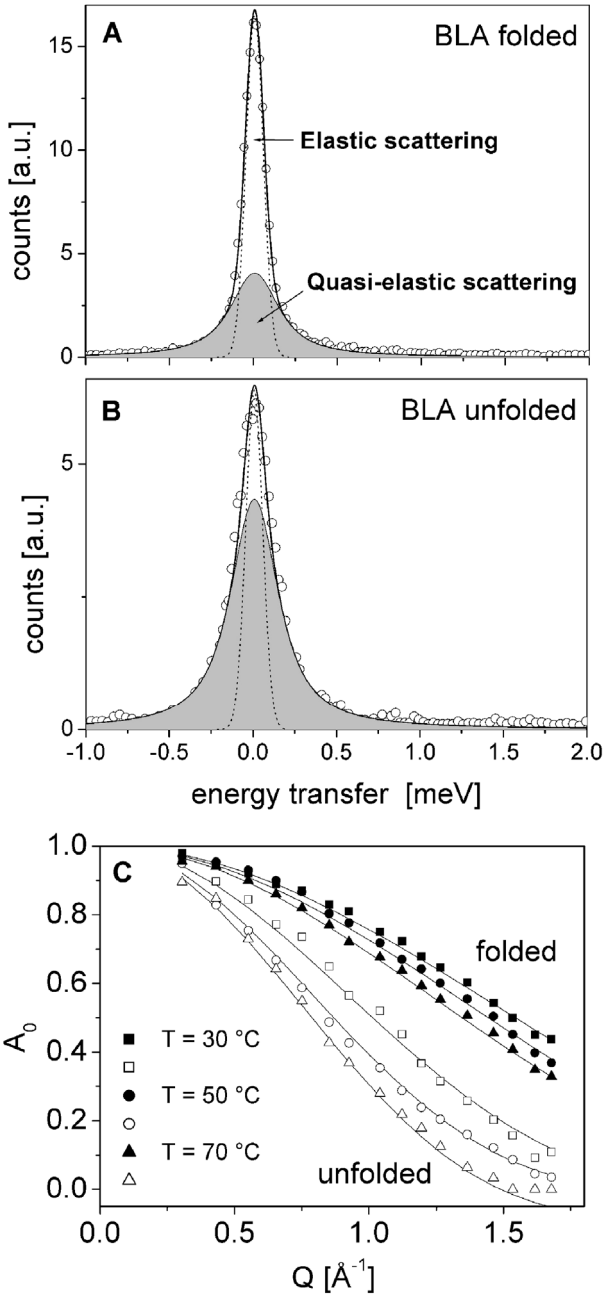

Figure 8. Energy transfer spectra as measured with neutron spectroscopy for BLA for the folded (*A*) and unfolded (*B*) state. The shaded area represents quasielastic scattering caused by internal structural fluctuations of the enzyme occurring in the picosecond time regime. The corresponding normalized elastic structure factors, A_0, are given for both states in the temperature range from 30 to 70 °C (data from [82]).

Conclusion and outlook

Many comparative studies on the thermostability of proteins in the last years have shown that thermostability occurs as a cumulative effect of many different, often rather small stabilizing features [5, 25]. Comparative studies with homologous α-amylases, which show an enormous variety of thermostabilities, offer the possibility to study features responsible for the thermostability of a medium-sized multi-domain protein. For various α-amylases, proposals about putative stabilizing mechanisms have been described. The challenge is to figure out to what extent the specific mechanisms really contribute to individual thermostabilities. This holds not only for α-amylases but also for many other proteins. With respect to irreversible unfolding and to strong aggregation, as often observed for α-amylases, the situation for this multi-domain protein is even more difficult. In particular, reliable thermodynamic data and structural as well as dynamic characteristics of the unfolded states are very

difficult or even impossible to obtain. I have stated in this review that besides structural features of the native state and thermodynamic parameters, for example, in terms of stability curves, structural and dynamic features of the unfolded states can contribute significantly to thermostability. Therefore, alternative and more suitable approaches are required to overcome the problems related to aggregation of unfolded states.

At least two approaches can help to overcome this problem. First, fluorescence correlation spectroscopy (FCS) can be applied to protein concentrations down to ~0.1 nM, which should significantly reduce or even circumvent aggregation of unfolded states. This technique measures diffusion coefficients and has already been employed successfully in studies on unfolded proteins [83]. Second, studies with various proteins demonstrates that molecular chaperones can suppress aggregation of non-native or unfolded proteins [84, 85]. It has already been shown for TAKA-amylase that chaperones (GroES and GroEL from *Escherichia coli*) inhibit aggregation reactions that compete with correct (re-)folding [86]. The mild conditions of sol-gel encapsulation provide a further technique to separate single proteins in isolated voids to reduce aggregation of unfolded states [87]. Although these approaches have a number of limitations (e.g., limited temperature range) and would be applicable only for some of the relevant aspects, studies with homologous α-amylases using these techniques have great potential for progress in this field of application.

Acknowledgements. The author thanks G. Büldt for continuous support at his institute and C. Duy for valuable discussions.

1 Anfinsen C. B. (1973) Principles that govern the folding of protein chains. Science **181:** 223–230
2 Stetter K. O. (1999) Extremophiles and their adaptation to hot environments. FEBS Lett. **452:** 22–25
3 Madigan M. T. and Marrs B. L. (1997) Extremophiles. Sci. Am. **276:** 82–87
4 Feller G. and Gerday C. (2003) Psychrophilic enzymes: hot topics in cold adaptation. Nat. Rev. Microbiol. **1:** 200–208
5 Jaenicke R. and Bohm G. (1998) The stability of proteins in extreme environments. Curr. Opin. Struct. Biol. **8:** 738–748
6 Sterner R. and Liebl W. (2001) Thermophilic adaptation of proteins. Crit. Rev. Biochem. Mol. Biol. **36:** 39–106
7 Vieille C. and Zeikus G. J. (2001) Hyperthermophilic enzymes: sources, uses and molecular mechanisms for thermostability. Microbiol. Mol. Biol. Rev. **65:** 1–43
8 Cavagnero S., Debe D. A., Zhou Z. H., Adams M. W. and Chan S. I. (1998) Kinetic role of electrostatic interactions in the unfolding of hyperthermophilic and mesophilic rubredoxins. Biochemistry **37:** 3369–3376
9 Beadle B. M., Baase W. A., Wilson D. B., Gilkes N. R. and Shoichet B. K. (1999) Comparing the thermodynamic stabilities of a related thermophilic and mesophilic enzyme. Biochemistry **38:** 2570–2576
10 Lazaridis T., Lee I. and Karplus M. (1997) Dynamics and unfolding pathways of a hyperthermophilic and a mesophilic rubredoxin. Protein Sci. **6:** 2589–2605
11 Hollien J. and Marqusee S. (1999) A thermodynamic comparison of mesophilic and thermophilic ribonucleases H. Biochemistry **38:** 3831–3836
12 Kumar S., Tsai C. J. and Nussinov R. (2001) Thermodynamic differences among homologous thermophilic and mesophilic proteins. Biochemistry **40:** 14152–14165
13 Perl D. and Schmid F. X. (2002) Some Like it hot: the molecular determinants of protein thermostability. Chembiochem **3:** 39–44
14 Arnold F. H., Wintrode P. L., Miyazaki K. and Gershenson A. (2001) How enzymes adapt: lessons from directed evolution. Trends Biochem. Sci. **26:** 100–106
15 Motono C., Oshima T. and Yamagishi A. (2001) High thermal stability of 3-isopropylmalate dehydrogenase from *thermus Thermophilus* resulting from low deltaC(p) of unfolding. Protein Eng. **14:** 961–966
16 Shiraki K., Nishikori S., Fujiwara S., Hashimoto H., Kai Y., Takagi M. et al. (2004) Comparative analyses of the conformational stability of a hyperthermophilic protein and its mesophilic counterpart. Eur. J. Biochem. **268:** 4144–4150
17 Georlette D., Blaise V., Collins T., D'Amico S., Gratia E., Hoyoux A. et al. (2004) Some like it cold: biocatalysis at low temperatures. FEMS Microbiol. Rev. **28:** 25–42
18 Miyazaki K., Wintrode P. L., Grayling R. A., Rubingh D. N. and Arnold F. H. (2000) Directed evolution study of temperature adaptation in a psychrophilic enzyme. J. Mol. Biol. **297:** 1015–1026
19 Schmid F. X. (1998) Optical spectroscopy to characterize protein conformation and conformational changes. In: Protein Structure: A Practical Approach, pp. 261–297, Creighton T. E. (ed.), IRL Press, Oxford
20 Pace C. N. and Scholtz J. M. (1998) Measuring the conformational stability of a protein. In: Protein Structure: A Practical Approach, pp. 299–321, Creighton T. E. (ed.), IRL Press, Oxford
21 Shriver J. W., Peters W. B., Szary N., Clark, A. T. and Edmondson S. P. (2001) Calorimetric analyses of hyperthermophile proteins. Methods Enzymol. **334:** 389–422
22 Vogl T., Jatzke C., Hinz H. J., Benz J. and Huber R. (1997) Thermodynamic stability of annexin V E17G: equilibrium parameters from an irreversible unfolding reaction. Biochemistry **36:** 1657–1668
23 D'Amico S., Marx J. C., Gerday C. and Feller G. (2003) Activity-stability relationships in extremophilic enzymes. J. Biol. Chem. **278:** 7891–7896
24 Panasik N., Brenchley J. E. and Farber G. K. (2000) Distributions of structural features contributing to thermostability in mesophilic and thermophilic alpha/beta barrel glycosyl hydrolases. Biochim. Biophys. Acta **1543:** 189–201
25 Petsko G. A. (2001) Structural basis of thermostability in hyperthermophilic proteins, or 'there's more than one way to skin a cat'. Methods Enzymol. **334:** 469–478
26 Vihinen, M. and Mantsala, P. (1989) Microbial amylolytic enzymes. Crit. Rev. Biochem. Mol. Biol. **24:** 329–418
27 Sogaard M., Abe J., Martineauclaire M. F. and Svensson B. (1993) Alpha-amylases – structure and function. Carbohydrate Polymers **21:** 137–146
28 Svensson B. (1994) Protein engineering in the alpha-amylase family – catalytic mechanism, substrate-specificity and stability. Plant Mol. Biol. **25:** 141–157
29 MacGregor E. A., Janecek S. and Svensson B. (2001) Relationship of sequence and structure to specificity in the alpha-amylase family of enzymes. Biochim. Biophys. Acta **1546:** 1–20
30 Nielsen J. E. and Borchert T. V. (2000) Protein engineering of bacterial alpha-amylases. Biochim. Biophys. Acta **1543:** 253–274
31 Leveque E., Janecek S., Haye B. and Belarbi A. (2000) Thermophilic archaeal amylolytic enzymes. Enzyme Microb. Technol. **26:** 3–14

32 Savchenko A., Vieille C. and Zeikus J. G. (2001) Alpha-amylases and amylopullulanase from pyrococcus furiosus. Methods Enzymol. **330:** 354–363

33 Linden A. and Wilmanns M. (2004) Adaptation of class-13 alpha-amylases to diverse living conditions. Chembiochem **5:** 231–239

34 Violet M. and Meunier J. C. (1989) Kinetic study of the irreversible thermal denaturation of *Bacillus licheniformis* alpha-amylase. Biochem. J. **263:** 665–670

35 Feller G., d'Amico D. and Gerday C. (1999) Thermodynamic stability of a cold-active alpha-amylase from the antarctic bacterium *Alteromonas haloplanctis*. Biochemistry **38:** 4613–4619

36 Fukada H., Takahashi K. and Sturtevant J. M. (1987) Differential scanning calorimetric study of the thermal unfolding of taka-amylase A from *Aspergillus oryzae*. Biochemistry **26:** 4063–4068

37 Fitter J., Herrmann R., Dencher N. A., Blume A. and Hauss T. (2001) Activity and stability of a thermostable alpha-amylase compared to its mesophilic homologue: mechanisms of thermal adaptation. Biochemistry **40:** 10723–10731

38 Nielsen A. D., Pusey M. L., Fuglsang C. C. and Westh P. A. (2003) Proposed mechanism for the thermal denaturation of a recombinant *Bacillus halmapalus* alpha-amylase – the effect of calcium ions. Biochim. Biophys. Acta **1652:** 52–63

39 Tanaka A. and Hoshino E. (2002) Calcium-binding parameter of *Bacillus Amyloliquefaciens* alpha-amylase determined by inactivation kinetics. Biochem. J. **364:** 635–639

40 Brzozowski A. M., Lawson D. M., Turkenburg J. P., Bisgaard-Frantzen H., Svendsen A., Borchert et al. (2000) Structural analysis of a chimeric bacterial alpha-amylase. High-resolution analysis of native and ligand complexes. Biochemistry **39:** 9099–90107

41 Laderman K. A., Davis B. R., Krutzsch H. C., Lewis M. S., Griko Y. V., Privalov P. L. et al. (1993) The purification and characterization of an extremely thermostable alpha-amylase from the hyperthermophilic archaebacterium *Pyrococcus furiosus*. J. Biol. Chem. **268:** 24394–24401

42 Jorgensen S., Vorgias C. E. and Antranikian G. (1997) Cloning, sequencing, characterization and expression of an extracellular alpha-amylase from the hyperthermophilic archaeon *Pyrococcus furiosus* in *Escherichia coli* and *Bacillus Subtilis*. J. Biol. Chem. **272:** 16335–16342

43 Linden A., Mayans O., Meyer-Klaucke W., Antranikian G. and Wilmanns M. (2003) Differential regulation of a hyperthermophilic alpha-amylase with a novel (Ca,Zn) two-metal center by zinc. J. Biol. Chem. **278:** 9875–9884

44 Machius M., Wiegand G. and Huber R. (1995) Crystal structure of calcium-depleted *Bacillus licheniformis* alpha-amylase at 2. 2 A resolution. J. Mol. Biol. **246:** 545–559

45 Declerck N., Machius M., Chambert R., Wiegand G., Huber R. and Gaillardin C. (1997) Hyperthermostable mutants of *Bacillus licheniformis* alpha-amylase: thermodynamic studies and structural interpretation. Protein Eng. **10:** 541–549

46 Machius M., Declerck N., Huber R. and Wiegand G. (2003) Kinetic stabilization of *Bacillus licheniformis* alpha-amylase through introduction of hydrophobic residues at the surface. J. Biol. Chem. **278:** 11546–11553

47 Suzuki Y., Ito N., Yuuki T., Yamagata H. and Udaka S. (1989) Amino acid residues stabilizing a *Bacillus* alpha-amylase against irreversible thermoinactivation. J. Biol. Chem. **264:** 18933–18938

48 Savchenko A., Vieille C., Kang S. and Zeikus J. G. (2002) *Pyrococcus furiosus* alpha-amylase is stabilized by calcium and zinc. Biochemistry **41:** 6193–61201

49 Fitter J. and Haber-Pohlmeier S. (2004) Structural stability and unfolding properties of thermostable bacterial alpha-amylases: a comparative study of homologous enzymes. Biochemistry **43:** 9589–9599

50 Dong G., Vieille C., Savchenko A. and Zeikus J. G. (1997) Cloning sequencing and expression of the gene encoding extracellular alpha-amylase from *Pyrococcus furiosus* and biochemical characterization of the recombinant enzyme. Appl. Environ. Microbiol. **63**(9)**:** 3569–3576

51 Machius M., Declerck N., Huber R. and Wiegand G. (1998) Activation of *Bacillus licheniformis* alpha-amylase through a disorder $\rightarrow$ order transition of the substrate-binding site mediated by a calcium-sodium-calcium metal triad. Structure **6**(3)**:** 281–292

52 Nonaka T., Fujihashi M., Kita A., Hagihara H., Ozaki K., Ito S. et al. (2003) Crystal structure of calcium-free alpha-amylase from *Bacillus* sp. strain KSM-K38 (AmyK38) and its sodium ion binding sites. J Biol. Chem. **278:** 24818–24824

53 Daniel R. M. and Danson M. J. (2001) Assaying activity and assessing thermostability of hyperthermophilic enzymes. Methods Enzymol. **334:** 283–293

54 Becktel W. J. and Schellman J. A. (1987) Protein stability curves. Biopolymers **26:** 1859–1877

55 Lumry R. and Eyring H. (1954) Conformation changes of proteins. J. Phys. Chem. **58:** 110–120

56 Perl D., Welker C., Schindler T., Schroder K., Marahiel M. A., Jaenicke R. et al. (1998) Conservation of rapid two-state folding in mesophilic, thermophilic and hyperthermophilic cold shock proteins. Nat. Struct. Biol. **5:** 229–235

57 Mukaiyama A., Takano K., Haruki M., Morikawa M. and Kanaya S. (2004) Kinetically robust monomeric protein from a hyperthermophile. Biochemistry **43:** 13859–13866

58 Wittung-Stafshede P. (2004) Slow unfolding explains high stability of thermostable ferredoxins: common mechanism governing thermostability? Biochim. Biophys. Acta **1700:** 1–4

59 Tomazic S. J. and Klibanov A. M. (1988) Mechanisms of irreversible thermal inactivation of *Bacillus* alpha-amylases. J. Biol. Chem. **263:** 3086–3091

60 Tomazic S. J. and Klibanov A. M. (1988) Why is one *Bacillus* alpha-amylase more resistant against irreversible thermoinactivation than another? J. Biol. Chem. **263:** 3092–3096

61 Plaza del Pino I., Ibarra-Molero B. and Sanchez-Ruiz J. M. (2000) Lower kinetic limit to protein thermal stability: a proposal regarding protein stability in vivo and its relation with misfolding diseases. Proteins **40:** 58–70

62 Lakowicz J. R. (1999) Principles of Fluorescence Spectroscopy, Kluwer Academic, New York

63 Shortle D. and Ackerman M. S. (2001) Persistence of native-like topology in a denatured protein in 8 M urea. Science **293:** 487–489

64 Klein-Seetharaman J., Oikawa M., Grimshaw S. B., Wirmer J., Duchardt E., Ueda T. et al. (2002) Long-range interactions within a nonnative protein. Science **295:** 1719–1722

65 Robic S., Guzman-Casado M., Sanchez-Ruiz J. M. and Marqusee S. (2003) Role of residual structure in the unfolded state of a thermophilic protein. Proc. Natl. Acad. Sci. USA **100:** 11345–11349

66 Frauenfelder H., Sligar S. G. and Wolynes P. G. (1991) The energy landscapes and motions of proteins. Science **254:** 1598–1603

67 Rasmussen B. F., Stock A. M., Ringe D. and Petsko G. A. (1992) Crystalline ribonuclease A loses function below the dynamical transition at 220 K. Nature **357:** 423–424

68 Kay L. E. (1998) Protein dynamics from NMR. Nat. Struct. Biol. **5** Suppl**:** 513–517

69 Fitter J., Verclas S. A., Lechner R. E., Seelert H. and Dencher N. A. (1998) Function and picosecond dynamics of bacteriorhodopsin in purple membrane at different lipidation and hydration. FEBS Lett. **433:** 321–325

70 Somero G. N. (1975) Temperature as a selective factor in protein evolution: the adaptational strategy of 'compromise'. J. Exp. Zool. **194:** 175–188

71 Zavodszky P., Kardos J., Svingor A. and Petsko G. A. (1998) Adjustment of conformational flexibility is a key event in the thermal adaptation of proteins. Proc. Natl. Acad. Sci. USA **95:** 7406–7411
72 Tang K. E. S. and Dill K. A. (1998) Native protein fluctuations: the conformational–motion temperature and the inverse correlation of protein flexibility with protein stability. J. Biomol. Struct. Dyn. **16:** 397–411
73 Tsai A. M., Udovic T. J. and Neumann D. A. (2001) The inverse relationship between protein dynamics and thermal stability. Biophys. J. **81:** 2339–2343
74 Collins T., Meuwis M. A., Gerday C. and Feller G. (2003) Activity, stability and flexibility in glycosidases adapted to extreme thermal environments. J. Mol. Biol. **328:** 419–428
75 Georlette D., Damien B., Blaise V., Depiereux E., Uversky V. N., Gerday C. et al. (2003) Structural and functional adaptations to extreme temperatures in psychrophilic, mesophilic and thermophilic DNA ligases. J. Biol. Chem. **278:** 37015–37023
76 Fitter J. and Heberle J. (2000) Structural equilibrium fluctuations in mesophilic and thermophilic alpha-amylase. Biophys. J. **79:** 1629–1636
77 Hernandez G., Jenney F. E. Jr, Adams M. W. and LeMaster D. M. (2000) Millisecond time scale conformational flexibility in a hyperthermophile protein at ambient temperature. Proc. Natl. Acad. Sci. USA **97:** 3166–3170
78 Butterwick J. A., Patrick Loria J., Astrof N. S., Kroenke C. D., Cole R., Rance M. et al. (2004) Multiple time scale backbone dynamics of homologous thermophilic and mesophilic ribonuclease HI enzymes. J. Mol. Biol. **339:** 855–871
79 Colombo G. and Merz K. M. Jr (1999) Stability and activity of mesophilic subtilisin E and its thermophilic homolog: insights from molecular dynamics simulations. J. Am. Chem. Soc. **121:** 6895–68903
80 Bee M. (1988) Quasi-elastic Neutron Scattering, Adam and Hilger, Philadelphia
81 Fitter J., Lechner R. E. and Dencher N. A. (1999) Interactions of hydration water and biological membranes studied by neutron scattering. J. Phys. Chem. B. **103:** 8036–8050
82 Fitter J. (2003) A measure of conformational entropy change during thermal protein unfolding using neutron spectroscopy. Biophys. J. **84:** 3924–3930
83 Chattopadhyay K., Saffarian S., Elson E. L. and Frieden C. (2005) Measuring unfolding of proteins in the presence of denaturant using fluorescence correlation spectroscopy. Biophys. J. **88:** 1413–1422
84 Buchner J., Schmidt M., Fuchs M., Jaenicke R., Rudolph R., Schmid F. X. et al. (1991) GroE facilitates refolding of citrate synthase by suppressing aggregation. Biochemistry **30:** 1586–1591
85 Ellis R. J. (2003) Protein folding: importance of the Anfinsen cage. Curr. Biol. **13:** R881–R883
86 Kawata Y., Hongo K., Mizobata T. and Nagai J. (1998) Chaperonin GroE-facilitated refolding of disulfide-bonded and reduced taka-amylase A from *Aspergillus oryzae*. Protein Eng. **11:** 1293–1298
87 Gill I. and Ballesteros A. (2000) Bioencapsulation within synthetic polymers (part 1): sol-gel encapsulated biologicals. Trends Biotechnol. **18:** 282–296
88 Koradi R., Billeter M. and Wuthrich K. (1996) MOLMOL: a program for display and analysis of macromolecular structures. J. Mol. Graph. **14:** 51–132